# **RSC Advances**



## PAPER

View Article Online
View Journal | View Issue



Cite this: RSC Adv., 2025, 15, 44548

# An efficient transition metal-free indolylation on 6chloropurine ribonucleosides and photophysical studies of conjugated nucleosides

Samir K. Mondal, Sakshi Singh and Shantanu Pal \*\*D\*\*

Herein, we report an efficient transition-metal-free approach for C-C bond formation on modified nucleosides *via* two complementary pathways: (i) a Lewis acid-mediated protocol employing AlCl<sub>3</sub>, and (ii) a Brønsted acid-mediated approach using trifluoroacetic acid (TFA). Among these, the TFA-HFIP system emerged as the optimal condition for regioselective C6-heteroaryl functionalization of 6-chloropurine nucleosides through direct coupling with diverse indole derivatives. To demonstrate the synthetic versatility of this methodology, a benzenesulfonamide-conjugated 1,2,3-triazole hybrid nucleoside was synthesized and subsequently explored Suzuki coupling and *N*-arylation to afford purine-fused polycyclic nucleosides. Photophysical studies revealed that the hybrid nucleoside 14 exhibits significantly enhanced fluorescence relative to the parent compound 11n, while the highly conjugated derivatives 15 and 17 show pronounced photophysical properties.

Received 15th October 2025 Accepted 10th November 2025

DOI: 10.1039/d5ra07899g

rsc.li/rsc-advances

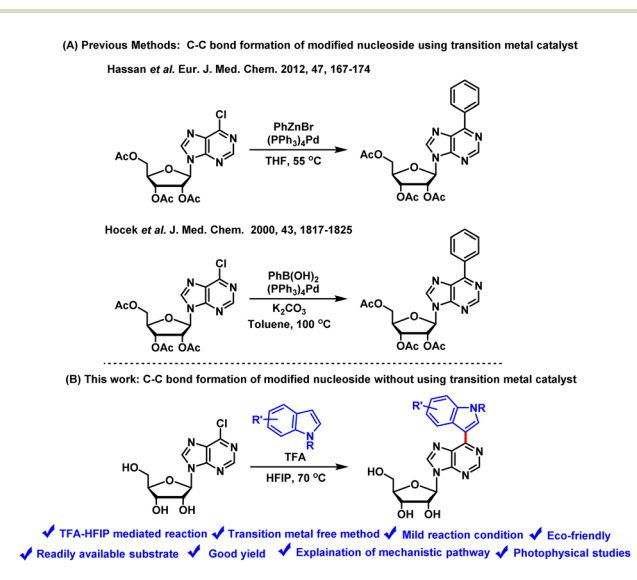
### Introduction

Biogenic purine nucleosides, as fundamental building blocks of DNA and RNA, play a crucial role in various biological processes.1 In medicinal chemistry, numerous drugs incorporating unnatural nucleosides or their analogues have been developed for the treatment of a wide range of diseases, including viral infections and cancers.2 Among these, purine nucleoside derivatives featuring various substituents (such as C, N, O, and S) at the C6 position have attracted significant attention due to their diverse biological activities, particularly their antitumor and cytotoxic effects.3 Consequently, the development of an efficient synthetic route to access novel C6heteroaryl purine nucleosides is of great significance in both organic and medicinal chemistry. To date, the synthesis of arylsubstituted purine nucleosides has predominantly relied on conventional methods involving transition metal-catalyzed cross-coupling reactions between aryl organometallic reagents (Ar-M) and 6-chloropurine nucleosides. For the synthesis of 6arylpurine nucleosides, various transition metal-catalyzed cross-coupling reactions, such as Suzuki-Miyaura,4 Stille,5 Negishi,6 and Kumada7 couplings have been extensively employed. While these methodologies have garnered considerable attention, they are often associated with several limitations: (a) the requirement for expensive transition metal catalysts such as palladium or nickel, often in combination with complex ligands to complete the catalytic cycle; (b) the need to prepare sensitive organometallic reagents under stringent

School of Basic Sciences, Indian Institute of Technology Bhubaneswar, Argul, Odisha, 752050, India. E-mail: spal@iitbbs.ac.in

conditions, including inert atmospheres; (c) generally low to moderate product yields; and (d) the use of hazardous or environmentally unfriendly solvents, *etc.* (Scheme 1). In this respect, the development of a transition metal-free approach represents a significant advancement, offering a more economical, sustainable, and operationally simple route for C–C bond formation on nucleosides.<sup>8</sup>

In 2010, the Guo group reported a method for the synthesis of aryl purines, utilizing a threefold aluminum chloride (AlCl<sub>3</sub>) to directly arylate 6-chloropurines with electron-rich arenes.<sup>9</sup>



Scheme 1 (A) Previously reported method and (B) present method.

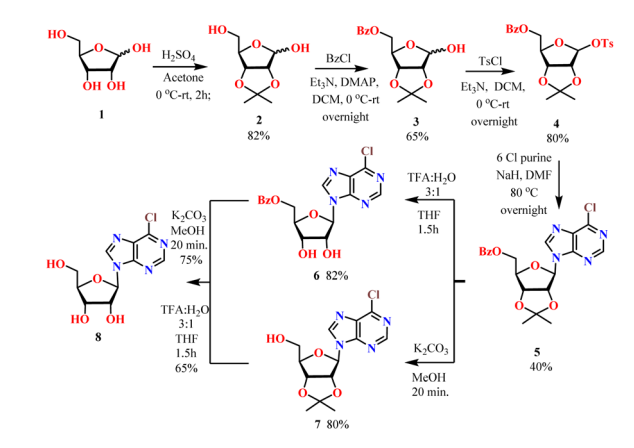
Paper

More recently, in 2019, Takenaga's group introduced an alternative approach for aryl purine synthesis, employing a combination of triflic acid and fluoro-alcohol to facilitate the direct arylation of 6-chloropurines, achieving the reaction in 24 hours.10 But the development of metal-free strategy for C-C bond formation on modified nucleosides remains a considerable challenge and, to the best of our knowledge, has not been previously reported. In this study, we report two transitionmetal-free approaches for C-C bond formation on purine nucleosides: (a) direct heteroarylation of 6-chloropurine with heteroarenes, catalyzed by anhydrous AlCl<sub>3</sub> as a Lewis acid, and (b) an alternative method employing trifluoroacetic acid. The comparative study highlights the distinct reactivity profiles of Lewis and Brønsted acids in activating the purine nucleoside scaffolds toward nucleophilic heteroarylation. To achieve efficient C-6 heteroarylation on modified nucleosides, we optimized the reaction conditions using the more affordable, commercially available TFA in HFIP as the solvent under heating condition for 12 hours. Further, we have demonstrated the synthetic utility of C6-heteroarylated nucleosides by successfully constructing a triazole-based hybrid nucleoside, thereby providing access to biologically relevant molecular frameworks. Due to this respect we attached benzenesulfonamide moiety to the C6-heteroarylated nucleoside via click chemistry which is a part of Prontosil drug used for antibiotic medicine.11 Additionally, compound 11q was subjected to Suzuki coupling reactions and N-arylated compound delivered the purine fused polycyclic nucleoside. Furthermore, the photophysical properties of the conjugated nucleosides were systematically investigated in a range of solvents to assess their solvatochromic behaviour and fluorescence characteristics.

#### Results and discussion

#### Chemistry

In light of our ongoing research on nucleoside chemistry<sup>12</sup> the development of new methods for synthesizing C-6 heteroarylated nucleoside analogues, we hypothesized that 6-chloropurine nucleoside could directly form a C-C bond with an electron-rich heteroaryl derivative without using any transition metal catalysts. In order to synthesize C-6 heteroarylation on modified nucleoside, p-ribose used as starting material. Initially, the 2,3-diol of D-ribose 1 was protected using acetone in the presence of a catalytic amount of sulfuric acid.<sup>13</sup> Subsequently, the primary hydroxyl group of the diol-compound 2 was protected with a benzoyl group.14 This was followed by the tosylation of the remaining secondary hydroxyl group under basic conditions in DCM, affording the fully protected intermediate 4.15 The tosylated compound 4 then underwent a nucleophilic substitution reaction with 6-chloropurine in the presence of sodium hydride in dry DMF,16 yielding the desired nucleoside compound 5 (Scheme 2). To optimize the reaction conditions for the metal-free synthesis of C6-heteroarylsubstituted purine nucleosides, compound 5 was initially subjected to a variety of reaction parameters. Based on previous literature report,9 compound 5 was reacted with three equivalents of AlCl<sub>3</sub> and an indole derivative in 1,2-dichloroethane



Scheme 2 Synthesis of intermediate nucleoside



Scheme 3 Indolylation on 6-Cl purine nucleoside.

(DCE) at 80 °C for 8 hours (Scheme 3). This reaction yielded a complex mixture of products, compounds 9, 10, and 7, along with unreacted starting material, as observed by TLC analysis. To drive the reaction to completion, the amount of AlCl<sub>3</sub> was increased to 3.5 equivalents while maintaining the same temperature.

Under this modified condition, the reaction was completed within 3-4 hours. However, the yield of the desired product remained low, possibly due to degradation of the sugar moiety in the presence of excess Lewis acid. Notably, the same set of three products (9, 10, and 7) were formed under this condition as well. All these products were isolated and characterized by NMR spectroscopy. To improve the yield of the desired compound 10, various reaction conditions were explored by modifying both the amount of Lewis acid (AlCl<sub>3</sub>) and the reaction temperature. Therefore, the AlCl<sub>3</sub> equivalence was reduced from 3.0 to 2.5 equivalents while maintaining the temperature at 80 °C. However, under these conditions, the reaction remained incomplete even after 24 hours and afforded only a minimal amount of desired product 10, as summarized the details studies in SI.

To overcome these challenges encountered under Lewis acid conditions, we turned our attention to Brønsted acid. In an effort to enhance both conversion and selectivity, we investigated fluorinated alcohols as solvents. Specifically, 1,1,1,3,3,3hexafluoro-2-propanol (HFIP) and 2,2,2-trifluoroethanol (TFE) were selected due to their unique physicochemical properties, including high polarity, moderate nucleophilicity, and strong hydrogen-bond donating ability characteristics that distinguish

them from non-fluorinated alcohols. Consequently, intermediate compound 5 was reacted with the indole derivative in HFIP using TFA as the Brønsted acid. This reaction led to the formation of the isopropyl-deprotected desired product 11d, along with the isopropyl-deprotected starting material 6. However, the overall yield of product 11d remained low, likely due to incomplete conversion and concurrent deprotection of the isopropylidene group during the reaction.

To improve efficiency and selectivity, we next employed the isopropyl-deprotected intermediate 6 directly in the transformation, likely due to the benzoyl protecting group in compound 6 effectively enhanced the stability of the sugar framework and promoted efficient C–C bond formation under Lewis acidic (TFA) conditions. When compound 6 was treated with the indole derivative in HFIP in the presence of 2 equivalents of TFA at room temperature, the desired C6- heteroarylated product 11d was obtained in 20% yield after 24 hours. Increasing the TFA three equivalents and raising the temperature to 50 °C under an inert atmosphere led to improve conversion, affording compound 11d in 50% yield after 24 hours.

Further increasing the TFA concentration to 3.5 equivalents and the temperature to 70 °C resulted in complete conversion within 12 hours, delivering product **11d** in 75% yield (Table 1). However, when the TFA amount was increased to 4 equivalents under otherwise identical conditions, decomposition of the sugar moiety was observed, and the yield of compound **11d** 

decreased to 50% (Table 1). To further improve the reaction outcome, mixed solvent systems such as HFIP/DCE and HFIP/ H<sub>2</sub>O were explored in the presence of three equivalents of TFA at 70 °C. In both cases, only trace amounts of the desired product were detected. The use of acetic acid as an alternative Brønsted acid in HFIP at 70 °C also failed to promote the reaction. Subsequently, we evaluated 2,2,2-trifluoroethanol (TFE) as an alternative fluorinated solvent under otherwise identical conditions. However, the reaction in TFE provided a lower yield (<30%) and was accompanied by the formation of colored impurities. Additional attempts using other solvents, including DCE and isopropanol, also failed to improve the yield. These results clearly indicate that both trifluoroacetic acid and the fluorinated alcohol solvent HFIP are essential for achieving efficient conversion in this C6-heteroarylation reaction. To gain further insight into the reaction mechanism and evaluate the generality of the transformation, the substrate scope was examined under the optimized reaction conditions (entry 8, Table 1). The direct C6-heteroarylation of 6-chloropurinemodified nucleoside with various non-N-protected indoles afforded the corresponding products (11a, 11b, 11e, 11f, and 11g) in moderate yields. Notably, indoles bearing electrondonating substituents reacted more efficiently, delivering the desired C6-arylated products (11b, 11c, 11d, 11e, 11f and 11h) in moderate to good yields.

These observations highlight the pronounced influence of electronic effects on the reactivity of heteroaryl nucleophiles in

Table 1 Optimization of the reaction condition<sup>a</sup>

Entry	Solvent	Additive	Temperature (°C)	Time (hour)	<b>11d</b> yield <sup>b</sup> (%)
1	TFA	_	Rt	12	Trace
2	TFA: H <sub>2</sub> O	_	Rt	12	<10
3	Pivalic acid	_	70	24	_
4	Pivalic acid	TFA (1 eq.)	70	24	_
5	CH₃COOH	_ ` ' ' '	70	24	_
6	HFIP	TFA (2 eq.)	Rt	24	20
7	HFIP	TFA (3 eq.)	50	24	50
8	HFIP	TFA (3.5 eq.)	70	12	75
9	HFIP	TFA (4 eq.)	70	12	50
10	HFIP + DCE(1:1)	TFA (3 eq.)	70	12	Trace
11	$HFIP + H_2O(1:1)$	TFA (3 eq.)	70	12	Trace
12	HFIP	CH₃COOH	70	12	_
13	2,2,2-TFE	TFA (3 eq.)	70	24	30
14	DCE	TFA (3 eq.)	70	24	_
15	Isopropanol	TFA (3 eq.)	70	24	_

<sup>&</sup>lt;sup>a</sup> Reaction conditions: 6 (1 mmol), Indole derivative (1.5 mmol), TFA (3.5 mmol), HFIP, 70 °C, 12 h <sup>b</sup> Isolated yield.

Scheme 4 Substrate scope of the reaction. Reaction Conditions: For 11a-i: compound 6' (1 mmol), Indole derivative (1.5 mmol), TFA (3.5 mmol), HFIP, 70 °C, 12h; 11j-t: compound 6' (1 mmol), indole derivative (1.5 mmol), TFA (3 mmol), HFIP, 50 °C, 16 h.

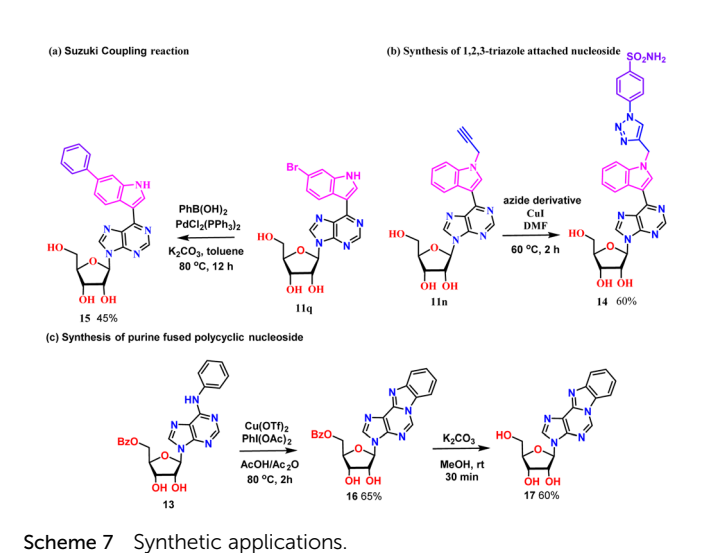
this transformation. In the case of 4-bromoindole, the strong electron-withdrawing effect of the bromine substituent significantly reduced the reactivity of the indole core, resulting in only trace amounts of the desired compound 11i, as confirmed by mass spectroscopy. Subsequently, we turned our attention to unprotected nucleosides. When the C-6 heteroarylation reaction was carried out under standard condition (entry 8, Table 1), these substrates underwent undesired  $\beta$ -glycosidic bond cleavage. To circumvent this issue, the reaction conditions were modified by reducing the amount of trifluoroacetic acid from 3.5 to 3 equivalents and lowering the temperature to 50 °C. Under this modified condition, the C6-heteroarylated products were obtained in slightly reduced yields compared to those obtained with benzoyl-protected nucleosides. The substrate scope was further explored using a variety of indole derivatives, including neutral, 5-OMe, 6-Br, 2-Ph, 2-Me, 5-Me, N-methylindole, etc. with a moderate yield of the corresponding products (Scheme 4). Indoles bearing electron-withdrawing groups, such as 5-nitroindole significantly reduced the reactivity of the indole core, failed to furnish the desired products under optimised condition. Additionally, the reaction with 6-bromoindole provided the desired product in lower yield, possibly due to electronic effects.

Scheme 5 Proposed mechanism via TFA-HFIP pathway.

Moreover, reactions using oxazole and thiazole as heteroaryl substrates were attempted; however, no reaction occurred. This lack of reactivity is likely due to the lower nucleophilicity of oxazole and thiazole compared to indole. We hypothesize that HFIP may enhance the acidity of TFA, which could increase the reactivity of the purine nitrogen atoms through hydrogen bonding with the fluoroalcohol. Furthermore, through hydrogen bonding and solvation, HFIP likely enhances the ability of the chloride atom to dissociate from the purine substrate, thereby promoting the formation of an activated intermediate. This intermediate could then undergo the aromatic substitution reactions. Based on the experimental observations and previous literature reports, 10 proposed mechanisms for the reaction under TFA conditions are outlined in Scheme 5. In the TFA-HFIP reaction medium, HFIP initially protonates the N1 position of purine A, affording the activated intermediate B. The resonance-stabilized negative charge at the C3 position of the indole subsequently attacks the C6 position of the purine ring, forming intermediate C. The elimination of chloride is facilitated through hydrogen-bonding interactions involving TFA and the HFIP anion, which also assist in the removal of a hydrogen atom to generate intermediate D. Finally, aromatization of the purine ring is promoted by the TFA anion, leading to the formation of the desired product 11j.

To illustrate the diversity of substrates and chemoselectivity of our reaction, we employed aniline and 4-methoxyaniline as a model substrate under the optimized condition (entry 8, Table 1). The reaction between compound 6 and aniline derivatives proceeded smoothly to afford the N-arylated products 12 and 13 in moderate yield, with no detectable formation of the Carylated isomers (such as 13') (Scheme 6), In contrast to indoles, which readily undergo electrophilic substitution at the C3-position due to their enhanced  $\pi$ -electron density, simple aromatic amines preferentially involve through nucleophilic attack of the nitrogen lone pair, thereby favouring N-arylation.

Scheme 6 TFA-mediated divergent product formation.



To further demonstrate the synthetic utility and broader applicability of the developed methodology, we designed and synthesized bioinspired hybrid nucleosides incorporating a tri-Prontosil-derived motif. azole-linked Accordingly, azidobenzenesulfonamide, a structural analogue of the prodrug Prontosil, was first prepared and subsequently employed in the coupling sequence to furnish the biologically relevant hybrid nucleoside scaffold. Thus, compound 11n was subjected to a copper(1)-catalyzed azide-alkyne cycloaddition with benzenesulfonamide azide in DMF, affording the triazole-linked hybrid nucleoside 14 in 60% yield (Scheme 7b).17 Furthermore, the bromo-substituted derivative compound 11q was employed to explore Suzuki,18 coupling reaction successfully yielding the corresponding product 15 (Scheme 7a). Additionally, the Narylated product 13 underwent a copper-catalyzed intramolecular amination, employing PhI(OAc)2 as a mild oxidant, to afford the purine-fused polycyclic nucleoside 16.19 Subsequent deprotection of the benzoyl group using K2CO3 in methanol furnished the corresponding unprotected purine-fused polycyclic nucleoside 17(Scheme 7c).

#### Photophysical studies

The photophysical properties of the fluorescent intermediate nucleoside **11n** and the hybrid nucleoside **14** were studied. UV-visible absorption and fluorescence emission spectra were recorded for both compounds in various organic solvents, including dichloromethane (DCM), ethanol (EtOH), methanol (MeOH), dimethylformamide (DMF), and dimethyl sulfoxide (DMSO), at a concentration of  $5 \times 10^{-6}$  mol L<sup>-1</sup> (Table 2).

Table 2 Photophysical properties of the compound 11n (5  $\times$  10<sup>-6</sup> mol L<sup>-1</sup>)

Solvent	$\lambda_{abs}^{\max a}(nm)$	$\lambda_{\mathrm{em}}^{\max b} (\mathrm{nm})$	$\operatorname{Log} \varepsilon$	Stocks shift (nm)	$\Phi_{ m F}^{\;\;c}$
DCM	336	387	3.6	51	0.258
EtOH	338	408	4.5	70	0.14
MeOH	346	403	4.8	57	0.19
DMF	347	386	4.7	39	0.177
DMSO	340	386	4.5	46	0.19

<sup>a</sup> Absorption maxima. <sup>b</sup> Emission maxima. <sup>c</sup> Fluorescence quantum yield determined by taking quinine sulfate in 0.5 M H<sub>2</sub>SO<sub>4</sub> ( $\Phi_{\rm F}=0.546$ ) as reference. Stokes shift = ( $\lambda_{\rm em}-\lambda_{\rm abs}$ ) nm.

UV-visible absorption studies revealed that compounds **11n** and **14** exhibit absorption bands in the range of 310–360 nm. These bands display two to three distinct peaks, which can be attributed to  $\pi$ - $\pi$ \* and n- $\pi$ \* charge transfer transitions. The fluorescence emission spectra of compounds **11n** and **14** in various solvents are presented in Fig. 1, and 2 respectively. The fluorescence quantum yields of the **1,2,3**-triazole-linked nucleoside hybrid product **14** in different solvents are significantly enhanced compared to the intermediate C6-heteroaryl nucleoside compound **11n** (Table 3).

This enhancement is attributed to the increased conjugation by introducing 1,2,3-triazole moiety and the benzenesulfonamide group, which extend the  $\pi$ -conjugation of the system.

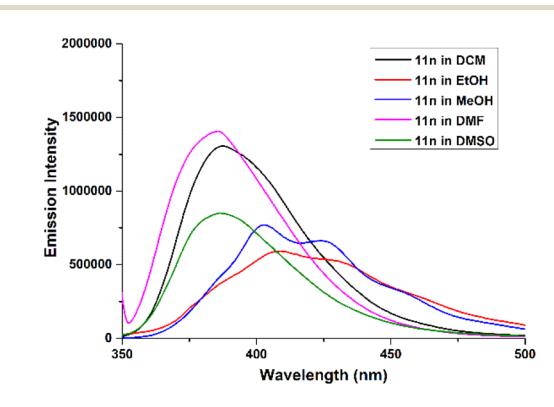


Fig. 1 Emission spectra in various organic solvents for compound 11n.

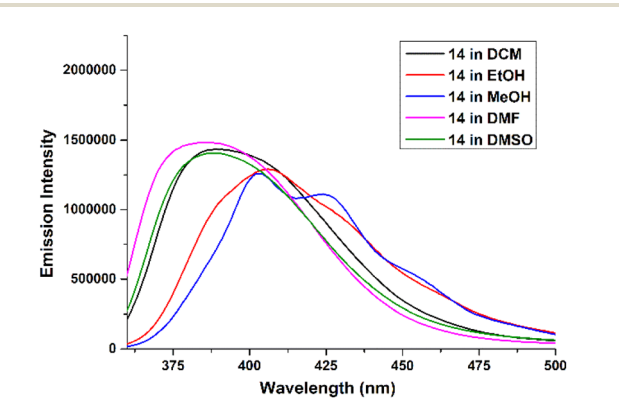


Fig. 2 Emission spectra in various organic solvents for compound 14.

Table 3 Photophysical Properties of the compound 14 (5  $\times$  $10^{-6} \text{ mol } L^{-1}$ 

Solvent	$\lambda_{\rm abs}^{\rm max}$ <sup>a</sup> (nm)	$\lambda_{\text{em}}^{\max b} (\text{nm})$	$\operatorname{Log} \varepsilon$	Stocks shift (nm)	$\Phi_{ ext{F}}^{}c}$
DCM	327	388	4.6	61	0.34
EtOH	348	406	4.4	58	0.39
MeOH	350	402	4.3	52	0.26
DMF	350	384	4.6	34	0.21
DMSO	351	387	3.7	36	0.213

<sup>&</sup>lt;sup>a</sup> Absorption maxima. <sup>b</sup> Emission maxima. <sup>c</sup> Fluorescence quantum yield determined by taking quinine sulfate in 0.5 M  $H_2SO_4$  ( $\Phi_F =$ 0.546) as reference. Stokes shift =  $(\lambda_{em} - \lambda_{abs})$  nm.

Table 4 Photophysical properties of the compound 15 (5  $\times$  $10^{-6} \text{ mol L}^{-1}$ 

Solvent	$\lambda_{\rm abs}^{\rm max\ \it a}$ (nm)	$\lambda_{\mathrm{em}}^{\max b} (\mathrm{nm})$	$\log \varepsilon$	Stocks shift (nm)	$\Phi_{ m F}^{\;\;c}$
DCM	330	4tpgoto "01	4.3	71	0.416
EtOH	340	432	3.82	92	0.30
MeOH	340	412	3.9	72	0.65
DMF	342	432	4	90	0.62
DMSO	342	412	4.08	70	0.30

<sup>&</sup>lt;sup>a</sup> Absorption maxima. <sup>b</sup> Emission maxima. <sup>c</sup> Fluorescence quantum yield determined by taking quinine sulfate in 0.5 M  $H_2SO_4$  ( $\Phi_F$  = 0.546) as reference. Stokes shift =  $(\lambda_{em} - \lambda_{abs})$  nm.

Both compounds 11n and 14 exhibited blue fluorescence emission, with compound 11n showing a quantum yield of 0.258 in DCM and compound 14 displaying a higher quantum yield of 0.390 in EtOH.

Further, the photophysical properties of compounds 15 and 17 were investigated in dichloromethane (DCM), ethanol (EtOH), methanol (MeOH), dimethylformamide (DMF), and dimethyl sulfoxide (DMSO), at a concentration of 5 ×  $10^{-6} \text{ mol L}^{-1}$  (Table 4).

Due to high conjugation of compounds 15 and 17 show the UV-visible absorption bands in the range of 250-450 nm and emission range 350-550, featuring to  $\pi$ - $\pi$ \* and n- $\pi$ \* chargetransfer transitions. The corresponding fluorescence emission

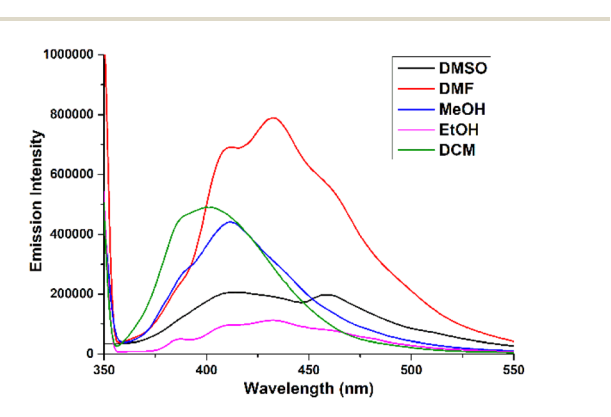


Fig. 3 Emission spectra in various organic solvents for compound 15.

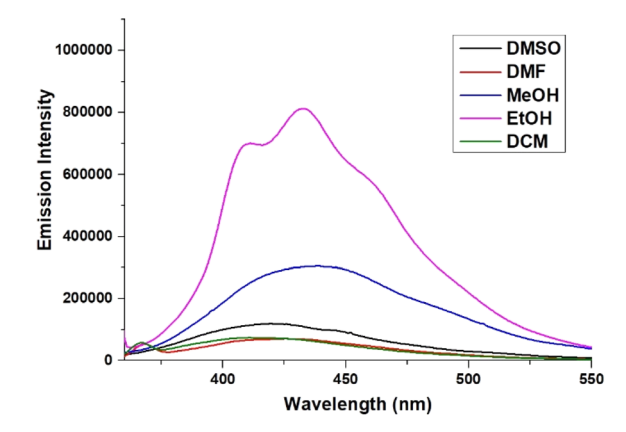


Fig. 4 Emission spectra in various organic solvents for compound 17.

Table 5 Photophysical Properties of the compound 17 (5  $\times$  $10^{-6} \text{ mol L}^{-1}$ 

Solvent	$\lambda_{abs}^{\max a} (nm)$	$\lambda_{\mathrm{em}}^{\max b} (\mathrm{nm})$	$\operatorname{Log} \varepsilon$	Stocks shift (nm)	$\Phi_{ m F}^{c}$
DCM	417	422	3.86	5	0.214
EtOH	390	433	4.45	43	0.60
MeOH	304	435	4.18	131	0.380
DMF	332	420	3.86	88	0.141
DMSO	291	420	4	129	0.339

<sup>&</sup>lt;sup>a</sup> Absorption maxima. <sup>b</sup> Emission maxima. <sup>c</sup> Fluorescence quantum yield determined by taking quinine sulfate in 0.5 M  ${
m H_2SO_4}$  ( $\Phi_{
m F}$  = 0.546) as reference. Stokes shift =  $(\lambda_{em} - \lambda_{abs})$  nm.

spectra of compounds 15 and 17 in different solvents are illustrated in Fig. 3 and 4, respectively (Table 5).

Compounds 15 and 17 displayed intense blue fluorescence in MeOH and ethanol with remarkable quantum yields of 0.65 and 0.60, respectively.

## Conclusions

In summary, we have developed an efficient and practical metalfree coupling strategy for the synthesis of C6-heteroarylsubstituted purine nucleosides via TFA-HFIP mediated activation. In contrast to the poor yields and low selectivity obtained with the Lewis acid AlCl<sub>3</sub>, the use of TFA in HFIP enabled a mild, selective, and high-yielding direct nucleophilic heteroarylation of purine-modified nucleosides. Overall, the present method provides a straightforward, and versatile approach for accessing a wide range of structurally diverse nucleoside analogues, representing a valuable contribution to sustainable nucleoside synthesis. Furthermore, the synthetic versatility of this methodology was demonstrated through the synthesis of a bioinspired triazole-linked hybrid nucleoside employing a benzenesulfonamide azide derived from the Prontosil drug scaffold. Subsequent Suzuki coupling and N-arylation reactions furnished a purine-fused polycyclic nucleoside, underscoring the adaptability of this approach. The successful synthesis of these biologically relevant scaffolds highlights the potential as

a valuable tool in medicinal chemistry and nucleoside-based drug discovery. Moreover, systematic photophysical studies in a range of solvents revealed distinct solvatochromic and fluorescence behaviors, further underscoring the potential functional versatility of the conjugated nucleosides.

### Conflicts of interest

The author declare no conflict of interest.

## Data availability

The authors confirm that the data supporting this article have been included as part of the supplementary information (SI). Supplementary information is available. See DOI: https://doi.org/10.1039/d5ra07899g.

## Acknowledgements

This research work is financially supported by the Ministry of Earth Science (MoES) (Sanction letter Number: MoES/PAMC/DOM/181/2023(E14616)) is greatly acknowledged.

#### Notes and references

- 1 Z. He, Y. Chen, Y. Wang, J. Wang, J. Mo, B. Fu, Z. Wang, Y. Du and X. Zhou, *Chem. Commun.*, 2016, 52, 8545.
- 2 (a) L. P. Jordheim, D. Durantel, F. Zoulim and C. Dumontet, Nat. Rev. Drug Discovery, 2013, 12, 447–464; (b) E. DeClercq, Annu. Rev. Pharmacol. Toxicol., 2011, 51, 1; (c) E. D. Clercq and A. Holy, Nat. Rev. Drug Discovery, 2005, 4, 928.
- 3 (a) M. Legraverend and D. S. Grierson, *Bioorg. Med. Chem.*, 2006, **14**, 3987–4006; (b) A. K. Bakkestuen, L. L. Gundersen and B. T. Utenova, *J. Med. Chem.*, 2005, **48**, 2710–2723; (c) Y. Murti, N. Badal and D. Pathak, *Int. Pharm. Sci.*, 2011, **1**, 116–122.
- 4 (a) M. Hocek, A. Holy, I. Votruba and H. Dvorakova, *J. Med. Chem.*, 2000, 43, 1817–1825; (b) S. Singh and S. Pal, *Chem. Commun.*, 2023, **59**, 13498.
- 5 (a) M. Havel, D. Dvorak and M. Hocek, *Tetrahydron*, 2002, 58, 7431–7435; (b) K. H. Shaughnessy, *Molecules Rev.*, 2015, 20, 9419–9454.
- 6 (a) A. M. Chacko, W. Qu and H. F. Kung, *J. Org. Chem.*, 2008, 73, 4874–4881; (b) C. W. Wang, H. Y. Niu, G. R. Qu, L. Liang, X. J. Wei, Y. Zhang and H. M. Guo, *Org. Bimol. Chem.*, 2011, 9, 7663.

- 7 (a) A. L. Krasovskiy, S. Haley, K. Voigtritter and B. H. Lipshutz, *Org. Lett.*, 2014, 16, 4066–4069; (b) A. R. Ankireddy, K. Paidikondala, R. Syed, R. Gundla, C. V. R. Reddy and T. Ganapathi, *Russ. J. Gen. Chem.*, 2020, 90, 1507–1517.
- (a) D. Bansal, G. Nataraj, C. Elanchezhian, P. Sivaganesan,
   M. K. Das and S. Chaudhuri, *Chem.-Asian J.*, 2025, 20,
   e202401437; (b) Z. Wang, L. Gan, Z. Song, Y. Liu and
   J. P. Wang, *Chin. J. Chem.*, 2024, 42, 3041-3046.
- 9 (a) H. M. Guo, P. Li, H. Y. Niu, D. C. Wang and G. R. Qu, J. Org. Chem., 2010, 75, 6016-6018; (b) L. Milhau and P. J. Guiry, Synlett, 2011, 3, 383-385; (c) M. Pal, V. R. Batchu, K. Parasuraman and K. R. Yeleswarapu, J. Org. Chem., 2003, 68, 6806-6809.
- (a) N. Tekenga, T. Shoji, T. Menjo, A. Hirai, S. Ueda, K. Kikushima, T. Hanasaki and T. Dohi, *Molecules*, 2019, 24, 3812; (b) P. Kalaramma and A. Goswami, *J. Org. Chem.*, 2021, 86(14), 9317–9327.
- 11 (a) Y. X. Chen, C. H. Chang, C. W. Li, J. J. Chen and T. L. Shih, *Chemistryselect*, 2023, 70, 1924–1936; (b) A. J. Almalki, T. S. Ibrahim, E. S. Taher, M. F. A. Mohammed, M. Youns, W. A. H. Hegazy and A. M. M. Al-Mahmoudy, *Molecules*, 2022, 27, 671.
- (a) S. K. Mondal and S. Pal, Eur. J. Org Chem., 2025, 28, e202500203;
   (b) B. Shivakrishna, S. Islam, A. Panda, M. Saranya, M. K. Santra and S. Pal, Anti-Cancer Agents in Med. Chem., 2018, 18, 1425-1431.
- 13 (a) B. Shivakrishna, S. Sahoo, A. Kumar and S. Pal, Chemistryselect, 2022, 7, e202203346; (b) S. N. Momm and R. Bruckner, J. Org. Chem., 2022, 87, 15415–15420.
- 14 J. Porter, M. A. Lima, I. Pongener and G. J. Miller, *Crbohydr. Res.*, 2023, 524, 108759.
- 15 G. Tanabe, Y. Manse, T. Ogaya, N. Sonoda, S. Marumoto, F. Ishikawa, K. Ninomiya, S. Chaipech, Y. Pongpiriyadacha, O. Muraoka and T. Morikawa, *J. Org. Chem.*, 2018, 83, 8250–8264.
- 16 D. Fushihara, H. Fukuda, H. Abe and S. Shuto, *Nucleotides Nucleic Acids*, 2019, **38**, 921–941.
- 17 J. E. Hein, J. C. Tripp, L. B. Krasnova, K. B. Sharpless and V. V. Fokin, *Angew. Chem., Int. Ed.*, 2009, 48, 8018–8021.
- 18 L. Li, S. Zhao, A. Joshi-Pangu, M. Diane and M. R. Biscoe, *J. Am. Chem. Soc.*, 2014, **136**, 14027–14030.
- 19 G. R. Qu, L. Liang, H. Y. Niu, W. H. Rao, H. M. Guo and J. S. Fossey, *Org. Lett.*, 2012, 14, 4494–4497.